TECHNICAL MEMORANDUM

762

Understanding the ECMWF winter surface temperature biases over Antarctica

Emanuel Dutra, Irina Sandu, Gianpaolo Balsamo, Anton Beljaars, Helene Freville[1], Etienne Vignon[2,3], and Eric Brun[1]

Research Department

November 2015

(1) CNRM-GAME UMR3589, Météo-France and CNRS, Toulouse, France
(2) Université Grenoble Alpes, LGGE – UMR5183, 38000 Grenoble, France
(3) CNRS/UJF– Grenoble 1, Laboratoire de Glaciologie et Géophysique de l'Environnement,UMR5183

Also submitted to: The Cryosphere

European Centre for Medium-Range Weather Forecasts
Europäisches Zentrum für mittelfristige Wettervorhersage
Centre européen pour les prévisions météorologiques à moyen

Series: ECMWF Technical Memoranda

A full list of ECMWF Publications can be found on our web site under:
http://www.ecmwf.int/publications/

Contact: library@ecmwf.int

European Centre for Medium Range Weather Forecasts
Shinfield Park, Reading, Berkshire RG2 9AX, England

Abstract

In this study we evaluate several factors that could explain the warm bias of surface temperature, and to some extent 2-meters temperature, in the ECMWF model and ERA-Interim reanalysis over Antarctica during winter. The study is focused on the Polar night where the solar radiation and latent heat fluxes can be neglected. Four main changes, derived from the surface energy balance, were tested including (i) reduction of the snow thermal inertia, (ii) full decoupling of the skin layer from the surface; (iii) reduced roughness lengths and (iv) different stability functions for the transfer coefficients calculations in the surface layer. Different configurations were tested within the ECMWF Integrated Forecasts System (IFS) in short-range forecasts and in stand-alone surface-only simulations at South Pole station. It was found that the model underestimates strong radiative cooling events and this can be mainly associated with a too strong land-atmosphere coupling over glaciers. The reduction of the snow thermally active depth had a positive effect allowing the model to better represent those radiative cooling effects. The reduction of the roughness lengths and the different stability functions also result in further cooling in stand-alone mode, but their impact was not so pronounced in the coupled forecasts. In general, averaged over the Antarctic continent, the reduction of the snow thermal active depth leads to a cooling of 1 K. The reduction of the roughness lengths resulted in an additional cooling of about 1 K. Our results indicate that the representation of a fast time scale to the thermal exchanges between the atmosphere and the surface is beneficial, suggesting the potential of a multi-layer snow scheme.

1 Introduction

West Antarctic has been identified as one of the fastest-warming regions globally (Bromwich et al., 2013a), which is consistent with the increasing mass loss from the West Antarctic Ice Sheet (King et al., 2012). However, robust long-term meteorological observations are scarce throughout the Antarctic continent. Additionally, observations of atmospheric temperature made on the Antarctic Plateau can be warm biased due to solar radiation (Genthon et al., 2011).

Atmospheric reanalysis provide long-term estimates of the state of the atmosphere and surface. However, the reanalysis quality is dependent on the quality and quantity of observations used by the data assimilation systems and by the performance of the forecast model. Jones and Lister (2015) found that the ECMWF ERA-Interim reanalysis (hereafter ERAI, Dee et al., 2011) has a warm bias (up to 5 °C) as detected over inland stations on the Antarctic continent , and a cold bias at lower latitudes, i.e. between 65°S and 78°S (by up to 6 °C). Therefore, the ERAI near surface air temperatures should be used with caution to study climate trends and variability over Antarctica. Despite local biases, ERAI initial and lateral boundary conditions were used in a climatic downscaling study over Antarctica (van Wessem et al., 2015) with a good performance compared with observations, and were also found to provide the best skill for regional forecasts performed with the polar weather research and forecasting model (Bromwich et al., 2013b). In the same study, the authors also reported a cold summer and a warm winter bias in 2-meters air temperature forecasts in the regional forecasts.

In a recent study, Fréville et al. (2014), hereafter HF14 found large warm biases in ERAI surface temperature, locally reaching 9°C, when comparing to satellite estimates of land surface temperature from MODIS, throughout the Antarctic continent. These results are confirmed also for ERA-Interim/Land (Balsamo et al., 2015) where no surface data assimilation was active, confirming the surface bias is within the modelling components. The warm bias was also found for 2-meters temperature, consistent with the study of Jones and Harpham (2013) and using the HadCRUT4 dataset

as reference. This warm bias is more pronounced during the Polar night when temperatures reach values below -65 °C. These very cold temperatures are mainly driven by surface radiative cooling in non-cloudy stable boundary layers. The representation of such conditions is known to remain a challenge for weather and climate models (Holtslag et al., 2013).

HF14 also performed stand-alone simulations with the CROCUS snowpack model (Brun et al., 1992 ; Vionnet et al., 2012) forced with ERAI. In this configuration, CROCUS is forced by the near-surface atmospheric fields at each time step, and it does not feedback on the atmosphere. In these simulations, the warm biases in surface temperature were much smaller than in ERAI, The authors therefore suggested that the calculation of surface fluxes in ERAI could be responsible for the strong positive biases found with respect the MODIS dataset.

The encouraging results of HF14 with a detailed snowpack model motivated us to investigate more in detail the potential sources of the temperature biases over the Antarctic continent in the ECMWF IFS model. We focus only on the Polar night to limit the sources of error by neglecting the effects of solar radiation and surface albedo and focusing on stable boundary layer conditions (Connolley, 1996). The different processes considered are derived from the current formulation used to solve the surface energy balance over permanent snow areas (glaciers). Different model configurations are then tested in stand-alone mode and in short-range forecasts. The following section describes the different model configurations and simulations followed by the results discussion. The main conclusions are presented in the last section.

2 Methods

2.1 Model

The IFS is the operational weather forecast model used at ECMWF for a wide range of applications including medium-range forecasts, ensemble forecasts, seasonal forecasting and atmospheric reanalysis like ERAI. The land-surface component of the IFS, HTESSEL (Balsamo et al., 2011), represents the land-surface processes and provides the boundary conditions for the heat, moisture and momentum transfers with the atmosphere. At the interface with the atmosphere, each grid box is divided into up to 6 land tiles representing different land covers (e.g. bare ground, high/low vegetation, exposed snow, shaded snow and interception). The surface energy balance is computed independently for each tile prior to solving the soil and snow mass and energy balance. Permanent snow covered grid-points (glaciers) are described by two time-invariant characteristics: a constant snow mass of 10000 kg m^{-2} and a density of 300 kg m^{-3}. The water balance over these points is not considered as the snow mass is kept constant. Considering the time-scales covered by the IFS (up to seasonal forecasts) this simplification is acceptable. The energy balance is solved as for regular snow grid boxes, i.e. with the single snow layer module described by Dutra et al. (2010), except that the thermally active snow depth is restricted to 1 meter. The following sections describe in detail the main processes involved in the heat exchanges between the glaciers and the atmosphere as represented in the model, and explain the changes we made to explore the possible causes of the warm biases over Antarctica.

2.1.1 Surface energy balance

The modeled surface temperature (skin temperature, T_{sk}) characterizes the temperature at the interface between the surface and the atmosphere. The skin layer represents the top layer of the surface with no heat capacity that responds instantaneously to changes (e.g. radiative forcing). In the IFS, the surface energy balance is solved in each grid box for each tile. In the case of glaciers, only the snow tile is active, and for simplicity only that tile will be presented in the following description. The surface energy balance equation can be written as:

$$(1-\alpha)R_s + \varepsilon\left(R_T + \sigma T_{sk}^4\right) + H + LE = \Lambda_{sk}(T_{sk} - T_{sn}) \quad (1)$$

where R_s and R_T are the downward short-wave and long-ware radiation, respectively, α and ε surface albedo and emissivity, respectively, σ the Stefan-Bolzmann constant, H the sensible heat flux, LE the latent heat flux, Λ_{sk} the skin conductivity, and T_{sn} the temperature of the snow layer. Because of the short time scale associated with the skin layer, equation (1) is linearized for T_{sk} (H and LE also depend on T_{sk}) and solved implicitly together with the vertical turbulent transport in the boundary layer. The sensible heat flux is given by:

$$H = \rho_a c_p |U_L| C_H (T_L + g z_L / c_P - T_{sk}) \quad (2)$$

with $\rho_a$the air density, c_P the heat capacity of moist air, g the acceleration of gravity, $|U_L|, T_L, z_L$ the wind speed, temperature and height of the lowest model level and C_H the bulk transfer coefficient.

In the austral winter, or polar night, the surface energy balance over Antarctica can be simplified by neglecting the downward short-wave radiation and the latent heat flux. With these two assumptions and expanding the sensible heat flux the energy balance in (1) can be written as:

$$\varepsilon\left(R_T + \sigma T_{sk}^4\right) + \rho_a c_p |U_L| C_H (T_L + g z_L / c_P - T_{sk}) - \Lambda_{sk}(T_{sk} - T_{sn}) = 0 \quad (3)$$

The surface temperature evolution will be modulated by the equilibrium between the three terms of eq. (3). HF14 found relatively small biases of downward long-wave radiation for ERAI during the polar night at the South Pole. Therefore, we can restrict our focus to the remaining two terms of eq. (3): (i) the sensible heat flux and (ii) the surface heat flux ($S = \Lambda_{sk}(T_{sk} - T_{sn})$). In the following sections we describe several direct and indirect changes to the calculation of these fluxes that to explore the main causes of the current errors of the surface temperature and 2-meters temperature in the IFS over Antarctica.

2.1.2 Surface heat flux

The surface heat flux is explicitly formulated in the surface energy balance. This implies that T_{sn} comes from the previous time-step following the coupling strategy of Best et al. (2004) that provides a well-defined (universal) interface between atmosphere and land surface models. Only snow temperature has a prognostic evolution in glacier grid-points (snow mass and density are kept constant), being computed by the snow scheme (Dutra et al., 2010). The snow energy budget neglecting phase changes can be simply written as:

$$(\rho C)_{sn} D^*_{sn} \frac{\partial T_{sn}}{\partial t} = S - G$$
$$G = \frac{T_{sn} - T_1}{0.5 \frac{D^*_{sn}}{\lambda_{sn}} + 0.5 \frac{D_{soil1}}{\lambda_{soil}}} \quad (4)$$

where $(\rho C)_{sn}$ is the snow volumetric heat capacity, D^*_{sn} is the snow thermal depth (considered to be equal to 1 meter for glacier points) and *G* is the snow basal heat flux. The snow basal heat flux follows a resistance approach considering the difference between the snow temperature and the underlying first soil layer temperature (T_1) where λ_{sn} is the snow thermal conductivity, and λ_{soil} the thermal conductivity of the first soil layer with depth D_{soil1}. The soil c. We hypothesize that the use of 1 meter for the snow thermal depth leads to a large thermal inertia that can affect the ability of the model to represent fast processes. Furthermore, the coupling of the snow with the underlying soil via the snow basal heat flux could be considered unrealistic as it relies on the soil temperature evolution under glaciers. Therefore, we tested a new formulation (hereafter denoted by DSN) that neglects the snow basal heat flux (setting *G*=0) and changes the snow thermal depth to 10 cm ($D^*_{sn} = 0.1$). This reduces the snow thermal inertia and allows capturing the fast time-scales. This change allows us to explore, in the simplest possible way, the potential benefit of having a multi-layer snow scheme with a shallow top layer which is able to respond to the fast-time scales.

A more drastic approach to reduce the impact of the snow thermal inertia on the surface temperature is to fully decouple the skin layer from the underlying surface (hereafter COND). This was achieved by changing the skin conductivity from its current value of 7 W m^{-2} K^{-1} to a very small value ($\Lambda_{sk} \ll 1$). In this situation, the surface temperature only depends on the balance between the long-wave emission and the sensible heat flux:

$$\varepsilon\left(R_T + \sigma T^4_{sk}\right) = -\rho_a c_p |U_L| C_H (T_L + g z_L / c_P - T_{sk}) \quad (5)$$

2.1.3 Sensible heat flux

In the sensible heat flux formulation (eq. (2)) the transfer coefficient (C_H) for stable conditions, depends on the momentum and heat roughness lengths and on the stability functions proposed by Holtslag and De Bruin (1988). These functions have been recommended by Andreas (2002) for their physical consistency in the limit of very stable stratification and they have been used in several studies on the surface fluxes estimation in Antarctica (Town and Walden, 2009; van den Broeke et al., 2005). They depend on the normalized height $z_L/\mathcal{L}$ where $\mathcal{L}$ is the Monin-Obukhov length estimated via an iterative method based on the bulk Richardson number (further details can be found in the IFS documentation (IFS, 2014) and in the Appendix).

Following the suggestion of HF14 that part of the warm bias of the IFS over Antarctica could be associated with the surface transfer coefficients, we tested the stability functions used in their study for stable conditions (hereafter EXC). These stability functions follow Louis (1979) with the modifications of Mascart et al. (1995) to allow for a discrimination between the roughness lengths for momentum and temperature. These functions are used in modeling platform SURFEX (Masson et al., 2013) in which CROCUS is integrated.

The momentum and heat roughness over glaciers in the IFS are currently set to $z_M = 1.3 \times 10^{-3}$ and $z_H = 1.3 \times 10^{-4}$ m respectively. There is a large spread in observationally based estimates of roughness lengths for momentum in Antarctica obtained in different areas of the continent. This is caused by the surface heterogeneity (smooth blue ice to rough snow, (Bintanja and Van Den Broeke, 1995)), the strong dependency of the roughness to the wind direction on snow fields (Jackson and Carroll, 1978) and the presence of drifting snow (Gallée et al., 2001). Andreas (1987) developed a theoretical model which highlights the dependency of the ratio z_H/z_M over snow and ice covered surfaces to the roughness Reynolds number R^*. Cassano et al. (2001) evaluated different surface flux parameterizations over Antarctica finding that better estimates of surface fluxes were obtained when taking the roughness lengths of heat higher than for those for momentum. They hypothesise that this could be compensating the mixing processes that are not taken into account by the Monin-Obukhov theory (gravity wave activity). van den Broeke et al. (2005) showed that in the katabatic wind zone the near-surface regime is rough (high R^*, $z_H \ll z_M$) while on regions of the plateau with low wind the flow is smoother (R* between 10^{-2} and 1, $z_H \sim z_M$). In this study we test new values of roughness lengths characteristic of the inland Antarctic under a moderately rough regime. z_M is therefore taken equal to 1.0×10^{-4} m and z_H taken equal to $z_M/2$ (simulation called hereafter ROU). The aim of testing these values is to access the potential sensitivity of the results to these changes. A detailed optimization procedure could be used but such an approach is out of the scope of this study.

2.2 Simulations and data

Different model configurations were evaluated in stand-alone mode by performing point simulations at the South Pole station (90°S 0°E) and in short-range forecasts. The different model configurations and their acronyms are listed in *Table 1*. Several tests combining different configurations were also evaluated and are referred in the text as "config1"_"config2". For example DSN_ROU_EXC combines the changes in the snow thermal active layer (DSN), the new roughness lengths (ROU) and the new stability functions (EXC).

Table 1. Description of the simulations configurations.

Experiment	Configuration
CTR	Default configuration
DSN	Change of snow thermal depth from 1 m to 0.1 and *G=0* (see Eq. (4))
COND	Decouple the skin layer with $\Lambda_{sk} \ll 1$.
ROU	Change of momentum roughness from 1.3×10^{-3} to 1.0×10^{-4} and heat roughness from 1.3×10^{-4} to 5.0×10^{-5}
EXC	Transfer coefficients using the SURFEX stability functions in stable conditions

2.2.1 Stand-alone simulations

The stand-alone simulations (sometimes referred as offline) use the same land-surface scheme as the IFS but there is no interaction with the atmosphere. In this setup, the surface model simulates a single point by prescribing the lowest model level temperature, specific humidity, wind speed and surface pressure, the fluxes of solid and liquid precipitation and the downward long-wave and shortwave radiation. This forcing was extracted from the ERAI reanalysis and the simulations were carried out for

one year (2009). The simulations were performed for the South Pole station for which three datasets used by HF14 were available: (i) surface temperature observations derived from radiation of BSRN instrumentation (Baseline Surface Radiation Network), (ii) MODIS land surface temperature; and (iii) simulations using the CROCUS snowpack model.

2.2.2 Short-range forecast simulations

The forecasts simulations were performed with the current version of the IFS (CY41R1, operational since May 2015) with a T255 spectral horizontal resolution (about 0.7° in the grid point space) and with 137 vertical levels (lowest model level near 10 m from the surface). The simulations consist in a series of short-range forecasts initialized every day at 00UTC for August 2009 taking the initial conditions from ERAI. The results are presented as the monthly mean of forecast steps +12/18/24/30 hours.

3 Results

3.1.1 South Pole surface-only simulations

We start the evaluation of the stand-alone simulations performed for the South Pole station by comparing the simulated surface temperature with the BSRN observations. The scatter plots in Figure 1 only include data for August 2009 to restrict the comparison to the polar night. The current model version (CTR) is very similar to ERAI or ERAI/Land over Antarctica, showing a warm bias particularly for very cold observed temperature (below -65 °C, panel c and d of Figure 1). The shape of the scatter cloud, with a warm tail for cold temperatures, is also similar to the results of Jones and Harpham (2013) that compared ERAI 2-meter temperature with HadCRUT4.

The new roughness lengths (panel e) or transfer coefficients (panel f) reduce the overall warm bias, but do not correct the model tendency to overestimate very cold temperatures. The warm biases at very cold temperatures are however reduced in the simulations with reduced snow thermal depth (panel g) and fully decoupled skin layer (panel j). These results suggest that the coupling to the surface is the main cause for the warm biases at cold temperatures, during strong radiative cooling events. Combining the lower roughness or transfer coefficients to either the reduced snow thermal depth or skin decoupling have an incremental effect and result in a further reduction of the warm bias. Finally, the configurations including the lower roughness, transfer coefficients and snow thermal depth or skin decoupling (DSN_ROU_EXC and COND_ROU_EXC) lead to overall biases that are similar to those found for the MODIS data (panel a) and for the CROCUS simulations (panel b).

The temporal evolution of the simulated surface temperatures in the different model configurations (see Figure 2), illustrate the lowering of the temperature in DSN/COND simulations, and the additive impact of ROU and EXC. The snow basal heat flux in the CTR simulation is approximately 5 W m^{-2} (see Figure 3). Since this flux is based on the snow/soil heat transfer, the assumption made in the DSN simulation, that this flux is negligible is acceptable. However, in the DSN configuration we also neglect the heat fluxes between the different layers of the snow in the glacier. This is expected to have some impact as we neglect the memory of the past synoptic conditions. This could partially explain the large spread in the scatter plots compared to that obtained for the CROCUS simulations, which simulate the thermal evolution of several snow layers (Figure 1). The DSN and COND simulations tend to be similar but COND has more variability (as seen in the scatter plots of Figure 1). This was expected as in the COND configuration the surface temperature results from the equilibrium between the long-wave emission and the sensible heat flux. The surface heat flux (S) in COND is zero with some oscillations (see Figure 3)

on the timestep level (less than 2 W m^{-2}) resulting from the linearization of the energy balance equation using the previous time step skin temperature.

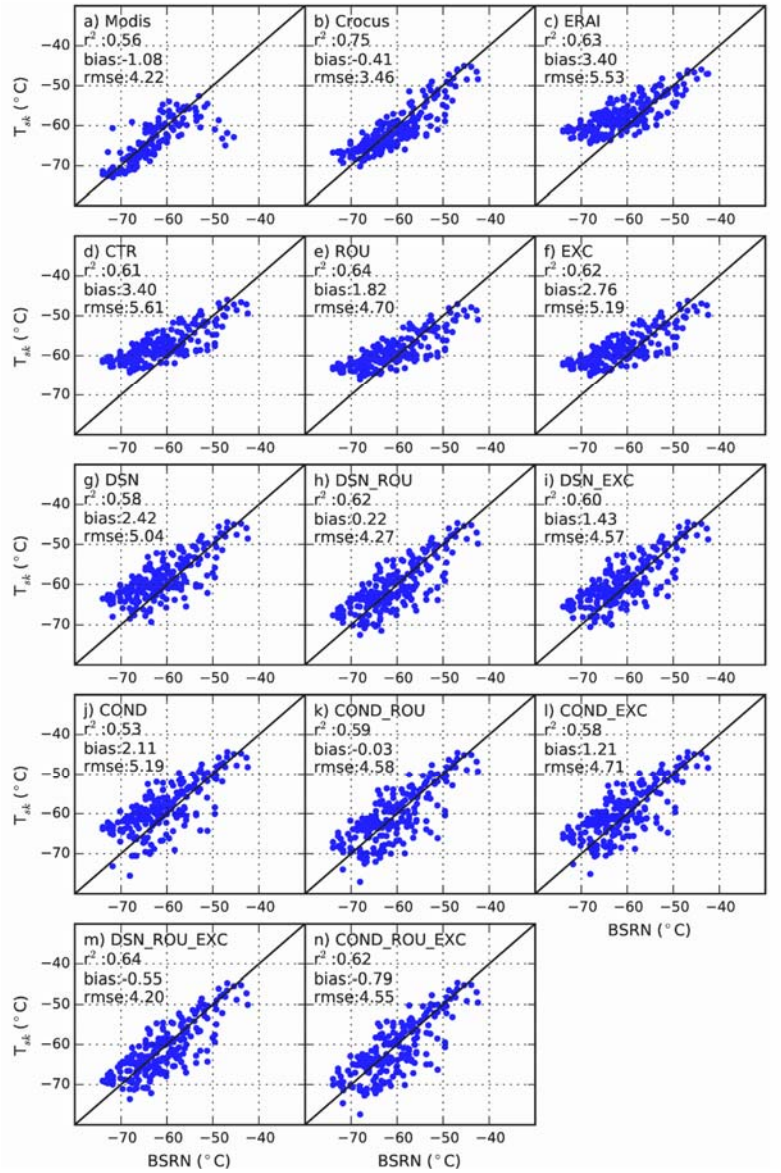

Figure 1. Scatter plots of surface temperature at the South Pole station from BSRN (horizontal axis) compared with (vertical axis) (a) MODIS, (b) CROCUS, (c) ERA-Interim, (d) control stand-alone simulation and (e to n) different stand-alone configurations during August 2009.

The temporal evolution of the heat and momentum transfer coefficients along with the Richardson number and wind-speed (see Figure 4) further highlight the different processes acting during the pronounced radiative cooling events. The reduction of snow thermal depth (DSN) leads to an increase of stability only during some events (e.g. on the 13th August 2009) that further reduces the transfer coefficients. On the other hand, the reduced roughness leads to a systematic reduction of both heat and momentum transfers coefficients. The different stability functions reduce the heat transfer coefficients, but slightly increase the momentum transfer coefficients (see also Figure S1 in the supplementary material). Only the DSN_ROU_EXC and COND_ROU_EXC were able to approach the very cold temperatures recorded around 9, 14 and 18 August (Figure 2), which are associated with low wind speed periods, and consequently very stable conditions. However, in the stand-alone simulations there is no

interaction with the atmosphere, so some of the results described in the section might be damped in coupled mode.

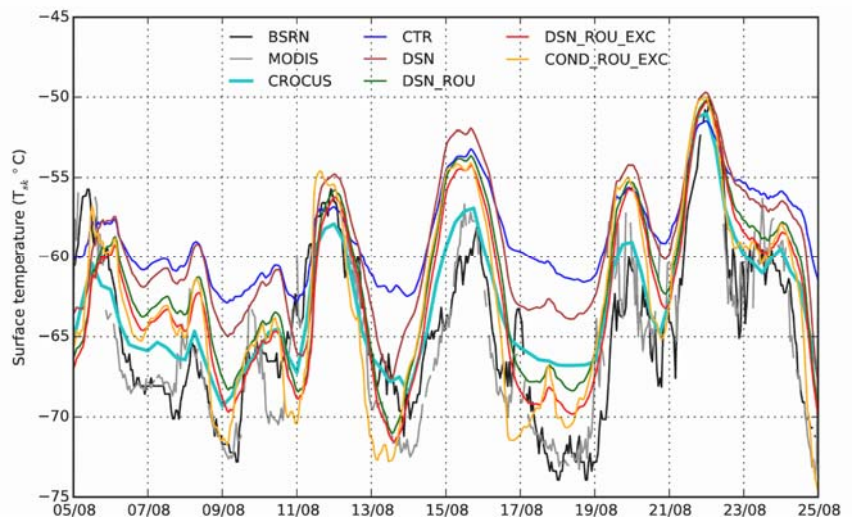

Figure 2. South Pole stand-alone surface temperature simulations compared with the BSRN (black), MODIS (grey) and CROCUS (thick cyan).

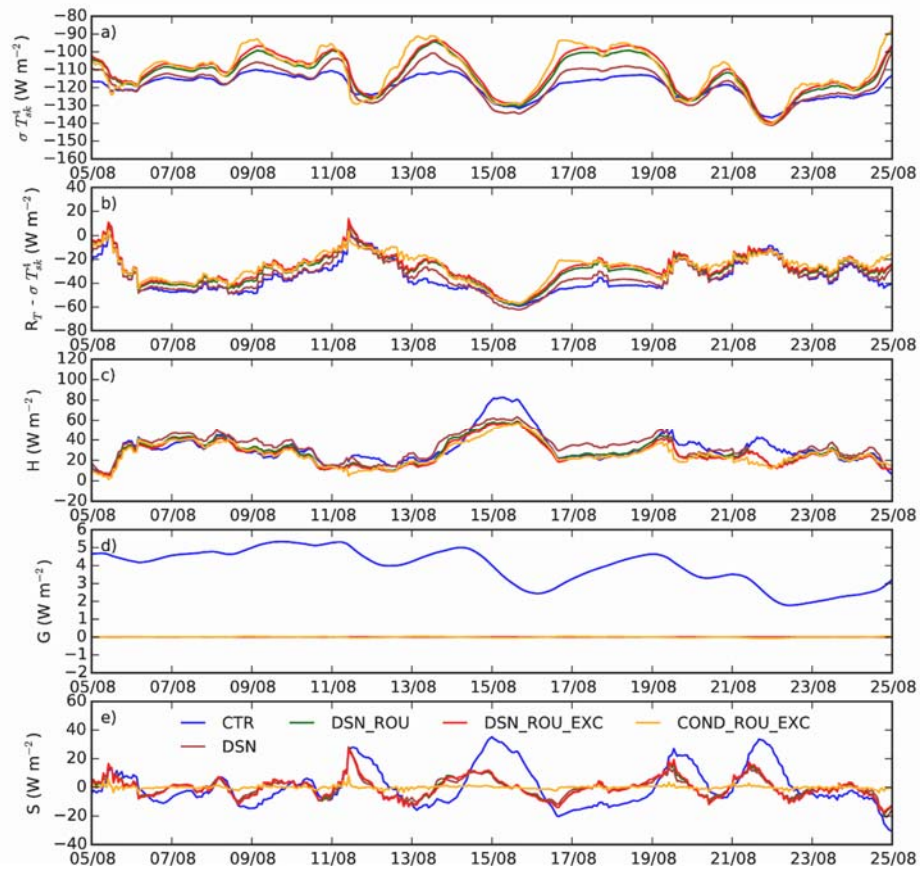

Figure 3. South Pole stand-alone simulations of (a) longwave emission, (b) net longwave radiation, (c) sensible heat flux, (d) ground heat flux and (e) surface heat flux.

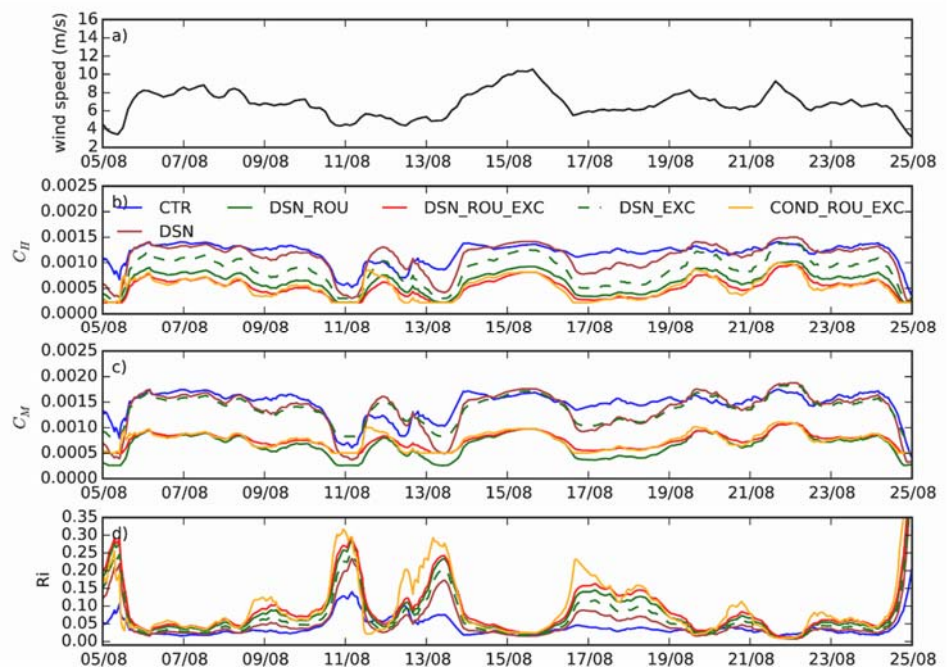

Figure 4. South Pole stand-alone (a) forcing wind speed and simulations of (b) heat transfer coefficient, (c) momentum coefficient and (d) Richardson number.

3.1.2 Forecasts with the coupled system

The reduction of the snow thermal depth leads to a cooling of the surface temperature in the coupled forecasts experiment (Figure 5) that reaches more than 4 K in some areas of Antarctica. The cooling is more pronounced in regions with a reduced cloud cover (see the mean cloud cover in Figure S2), as these regions are prone to pronounced radiative cooling events. The full decoupling of the skin layer (COND configuration) was not tested in coupled mode as it can lead to numerical instabilities and it would be unrealistic on the global scale. The reduction of the roughness lengths lead to a systematic cooling between 1 and 2 K, that is additive to the effect obtained from the reduction of the snow thermal depth. In the stand-alone simulations the reduction of the roughness length suggested a stronger impact. In the forecasts, the reduction of the roughness lengths leads to an increase of the wind-speed near the surface (see Figure S3) which enhances the turbulent mixing. This outweighs the impact of the roughness reduction on the turbulent heat flux. The changes in surface temperature are also seen in the 2-meters temperature (Figure S4) and in the lowest model level (Figure S5), but with a smaller amplitude.

The vertical profiles of temperature and wind-speed averaged over Antarctica (Figure 6) resume the above results, showing an average cooling of the surface of approximately 1 K, respectively 2 K, in the DSN and DSN_ROU experiments. The cooling impact is limited however to the first model level. These results suggest that the DSN and DSN_ROU configurations lead to a stronger land-atmosphere decoupling, that allows for stronger thermal gradients between the lowest model level and the surface. The wind profile in the DSN simulation is very similar to that in the CTR, while the roughness reduction leads to a general wind speed increase of about 1 m s^{-1} on average. This wind speed increase reduces with height, and is visible only in the lower troposphere (up to 900hPa).

Using different stability functions for the computation of the transfer coefficients (EXC) had only very small, close to neutral, impact when tested in combination with DNS and ROU configurations. Different

configurations, where we changed only the heat transfer coefficients, or both heat and momentum coefficients, also showed similar small impacts. In the stand-alone simulations the EXC configuration had a significant impact, but in coupled mode this was not the case, even when only the heat transfer coefficients were changed. This can be attributed to the atmospheric response that impacts the stability in the surface layer and does not lead to large Richardson numbers as in the stand-alone experiments.

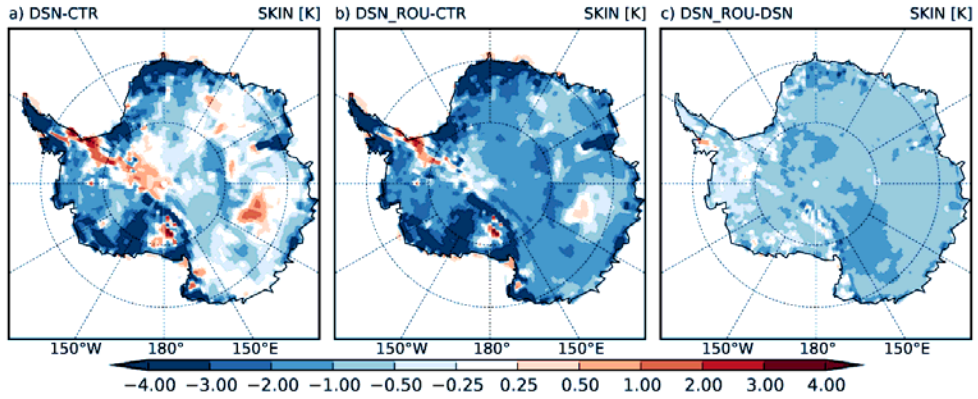

Figure 5. Impact on surface temperature in the forecast experiments for August 2009: (a) DSN-CTR, (b) DSN_ROU – CTR and (c) DSN_ROU – DSN.

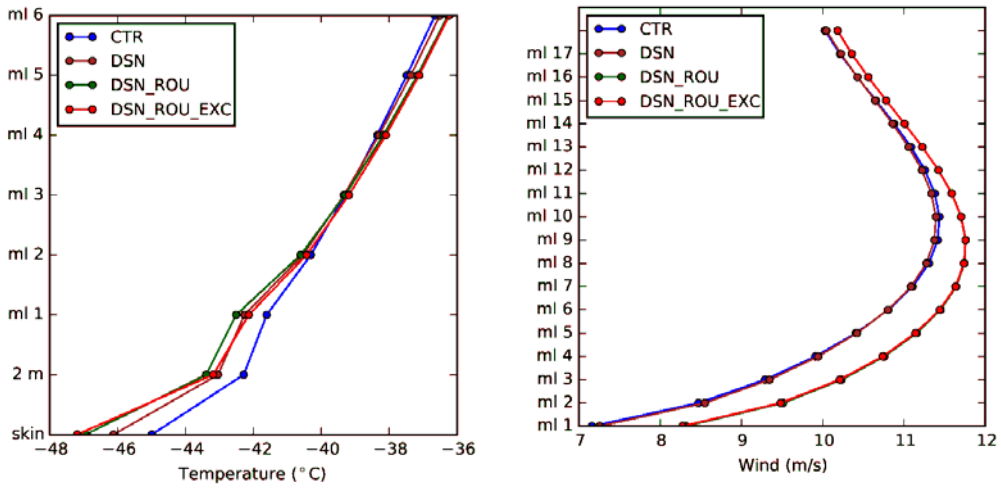

Figure 6. Vertical profiles of temperature (left) and wind speed (right) averaged over the Antarctica continent in the forecasts experiments for August 2009. The vertical axis indicate the model level as "ml #" and in the temperature profiles "skin" represents the surface layer and "2 m" the 2 meters level. Model levels #1,#6 and #17 are approximately 10, 120 and 1000 m above the surface.

4 Conclusions

In this study we evaluated several factors that could contribute to the large warm bias of surface temperature in ERAI and in forecasts performed with the ECMWF model over Antarctica during winter. The study is focused on the Polar night where the solar radiation and latent heat fluxes can be neglected. Four main changes were tested including (i) reduction of the snow thermal inertia, (ii) full decoupling of the skin layer from the surface; (iii) reduced roughness lengths and (iv) different stability functions

for the turbulent transfer coefficients. Several configurations were tested in stand-alone mode at the South Pole station, and in regular short-range forecasts, and compared with the recent findings of HF14.

It was found that the model tends to underestimate strong radiative cooling events and this can be mainly associated with a too strong land-atmosphere coupling over glaciers. The reduction of the snow thermal active depth from 1 m to 10 cm had a positive effect allowing the model to better represent those radiative cooling events. On the other hand, the enhanced decoupling between the surface and the atmosphere caused an overestimation of surface temperatures during warming periods in the stand-alone simulations. This could be partially due to biases in the forcing data extracted from ERAI, but could be also result from the simplified approach that neglects the heat transfer between the top snow layer and the remaining snow/ice layers.

The lower roughness lengths and the different stability functions had a cooling effect in the stand-alone simulations, but their impact was not so pronounced in coupled short-range forecasts. In general, averaged over the Antarctic continent, the reduction of the snow thermal active depth led to a cooling of 1 K, and when combined with the reduced roughness lengths resulted in a 2 K cooling. HF14 reported ERAI has biases of up to 6 K during the Polar night with respect to MODIS data. Our results indicate that it is necessary to represent the fast time scale in the thermal exchange between the atmosphere and the surface. This supports further developments toward the implementation of a multi-layer snow scheme. This is a necessary step before further evaluation of the remaining uncertainties associated with the surface roughness and turbulent exchange in stable conditions.

Acknowledgements

We thank Christophe Genthon and Patrick Le Moigne for the discussions related with the roughness lengths and the stability functions used in SURFEX.

Appendix: Transfer coefficients

Currently in the IFS the transfer coefficients for heat C_H and momentum C_M are expressed as:

$$C_H = \frac{\kappa^2}{\left[\log\left(\frac{z_L + z_{0M}}{z_{0M}}\right) - \Psi_M\left(\frac{z_L + z_{0M}}{\mathcal{L}}\right) + \Psi_M\left(\frac{z_{0M}}{\mathcal{L}}\right)\right]\left[\log\left(\frac{z_L + z_{0M}}{z_{0H}}\right) - \Psi_H\left(\frac{z_L + z_{0M}}{\mathcal{L}}\right) + \Psi_H\left(\frac{z_{0H}}{\mathcal{L}}\right)\right]}$$

$$C_M = \frac{\kappa^2}{\left[\log\left(\frac{z_L + z_{0M}}{z_{0M}}\right) - \Psi_M\left(\frac{z_L + z_{0M}}{\mathcal{L}}\right) + \Psi_M\left(\frac{z_{0M}}{\mathcal{L}}\right)\right]^2} \quad \text{(A1)}$$

where κ is the Von Karmann constant, z_L the lowest model level height (approximately 10 meters) and z_M, z_H the momentum and heat roughness, respectively. The stability profile functions Ψ for stable profiles are assumed to have the empirical forms proposed by Holtslag and De Bruin (1988). The profiles are given by:

$$\Psi_{\mathrm{M}}(\zeta) = -b\left(\zeta - \frac{c}{d}\right)exp(-d\zeta) - a\zeta - \frac{bc}{d}$$
$$\Psi_{\mathrm{H}}(\zeta) == -b\left(\zeta - \frac{c}{d}\right)exp(-d\zeta) - \left(1 + \frac{2}{3}a\zeta\right)^{1.5} - \frac{bc}{d} + 1 \quad \text{(A2)}$$

where *a=1*, *b=2/3*, *c=5* and *d=0.35*. The stability parameter $\zeta = z_L/\mathcal{L}$ is limited to 5 to allow the effect of a low critical Richardson number.

The SURFEX transfer coefficients follow the Louis (1979) formulation modified to consider different roughness lengths (Mascart et al., 1995) and for stable conditions are expressed as:

$$C_M = \frac{\kappa^2}{\left[log\left(\frac{z_L}{z_{0M}}\right)\right]^2\left[1 + \frac{10R_i}{\sqrt{1+5R_i}}\right]}$$
$$C_H = \frac{\kappa^2}{\left[\log\left(\frac{z_L}{z_{0M}}\right)\right]\left[\log\left(\frac{z_L}{z_{0H}}\right)\right]\left[1 + 15R_i\sqrt{1+5R_i}\right]} \quad \text{(A3)}$$

where R_i, is the Richardson number. In SURFEX the Richardson number is limited to 0.2.

The momentum and heat transfer coefficients as a function of the Richardson number are presented in the supplementary material (Figure S1) for the default roughness lengths ($z_M = 1.3 \times 10^{-3}$ and $z_H = 1.3 \times 10^{-4}$) and for lower roughness lengths ($z_M = 1.0 \times 10^{-4}$ and $z_H = 5.0 \times 10^{-5}$).

References

Andreas, E., 1987. A theory for the scalar roughness and the scalar transfer coefficients over snow and sea ice. Boundary-Layer Meteorol, 38(1-2): 159-184.

Andreas, E.L., 2002. Parameterizing Scalar Transfer over Snow and Ice: A Review. J. Hydrometeorol., 3(4): 417-432.

Balsamo, G. et al., 2015. ERA-Interim/Land: a global land surface reanalysis data set. Hydrol. Earth Syst. Sci., 19(1): 389-407.

Balsamo, G. et al., 2011. Evolution of land surface processes in the IFS. ECMWF Newsletter, 127: 17-22.

Best, M.J., Beljaars, A., Polcher, J. and Viterbo, P., 2004. A proposed structure for coupling tiled surfaces with the planetary boundary layer. J. Hydrometeorol., 5(6): 1271-1278.

Bintanja, R. and Van Den Broeke, M., 1995. Momentum and scalar transfer coefficients over aerodynamically smooth antarctic surfaces. Boundary-Layer Meteorol, 74(1-2): 89-111.

Bromwich, D.H. et al., 2013a. Central West Antarctica among the most rapidly warming regions on Earth. Nature Geosci, 6(2): 139-145.

Bromwich, D.H., Otieno, F.O., Hines, K.M., Manning, K.W. and Shilo, E., 2013b. Comprehensive evaluation of polar weather research and forecasting model performance in the Antarctic. J. Geophys. Res. Atmos., 118(2): 274-292.

Brun, E., David, P., Sudul, M. and Brunot, G., 1992. A Numerical-Model to Simulate Snow-Cover Stratigraphy for Operational Avalanche Forecasting. Journal of Glaciology, 38(128): 13-22.

Cassano, J.J., Parish, T.R. and King, J.C., 2001. Evaluation of Turbulent Surface Flux Parameterizations for the Stable Surface Layer over Halley, Antarctica*. Monthly Weather Review, 129(1): 26-46.

Connolley, W.M., 1996. THE ANTARCTIC TEMPERATURE INVERSION. International Journal of Climatology, 16(12): 1333-1342.

Dee, D.P. et al., 2011. The ERA-Interim reanalysis: configuration and performance of the data assimilation system. Quarterly Journal of the Royal Meteorological Society, 137(656): 553-597.

Dutra, E. et al., 2010. An Improved Snow Scheme for the ECMWF Land Surface Model: Description and Offline Validation. J. Hydrometeorol., 11(4): 899-916.

Fréville, H. et al., 2014. Using MODIS land surface temperatures and the Crocus snow model to understand the warm bias of ERA-Interim reanalyses at the surface in Antarctica. The Cryosphere, 8(4): 1361-1373.

Gallée, H., Guyomarc'h, G. and Brun, E., 2001. Impact Of Snow Drift On The Antarctic Ice Sheet Surface Mass Balance: Possible Sensitivity To Snow-Surface Properties. Boundary-Layer Meteorol, 99(1): 1-19.

Genthon, C., Six, D., Favier, V., Lazzara, M. and Keller, L., 2011. Atmospheric Temperature Measurement Biases on the Antarctic Plateau. Journal of Atmospheric and Oceanic Technology, 28(12): 1598-1605.

Holtslag, A.A.M. and De Bruin, H.A.R., 1988. Applied Modeling of the Nighttime Surface Energy Balance over Land. Journal of Applied Meteorology, 27(6): 689-704.

Holtslag, A.A.M. et al., 2013. Stable Atmospheric Boundary Layers and Diurnal Cycles: Challenges for Weather and Climate Models. Bulletin of the American Meteorological Society, 94(11): 1691-1706.

IFS, 2014. IFS Documentation CY40r1: IV Physical processes.

Jackson, B.S. and Carroll, J.J., 1978. Aerodynamic roughness as a function of wind direction over asymmetric surface elements. Boundary-Layer Meteorol, 14(3): 323-330.

Jones, P.D. and Harpham, C., 2013. Estimation of the absolute surface air temperature of the Earth. J. Geophys. Res. Atmos., 118(8): 3213-3217.

Jones, P.D. and Lister, D.H., 2015. Antarctic near-surface air temperatures compared with ERA-Interim values since 1979. International Journal of Climatology, 35(7): 1354-1366.

King, M.A. et al., 2012. Lower satellite-gravimetry estimates of Antarctic sea-level contribution. Nature, 491(7425): 586-589.

Louis, J.-F., 1979. A parametric model of vertical eddy fluxes in the atmosphere. Boundary-Layer Meteorol, 17(2): 187-202.

Mascart, P., Noilhan, J. and Giordani, H., 1995. A modified parameterization of flux-profile relationships in the surface layer using different roughness length values for heat and momentum. Boundary-Layer Meteorol, 72(4): 331-344.

Masson, V. et al., 2013. The SURFEXv7.2 land and ocean surface platform for coupled or offline simulation of earth surface variables and fluxes. Geosci. Model Dev., 6(4): 929-960.

Town, M.S. and Walden, V.P., 2009. Surface energy budget over the South Pole and turbulent heat fluxes as a function of an empirical bulk Richardson number. J. Geophys. Res. Atmos., 114(D22): D22107.

van den Broeke, M., van As, D., Reijmer, C. and van de Wal, R., 2005. Sensible heat exchange at the Antarctic snow surface: a study with automatic weather stations. International Journal of Climatology, 25(8): 1081-1101.

van Wessem, J.M. et al., 2015. Temperature and Wind Climate of the Antarctic Peninsula as Simulated by a High-Resolution Regional Atmospheric Climate Model. J. Clim., 28(18): 7306-7326.

Vionnet, V. et al., 2012. The detailed snowpack scheme Crocus and its implementation in SURFEX v7.2. Geosci. Model Dev., 5(3): 773-791.

Supplementary material

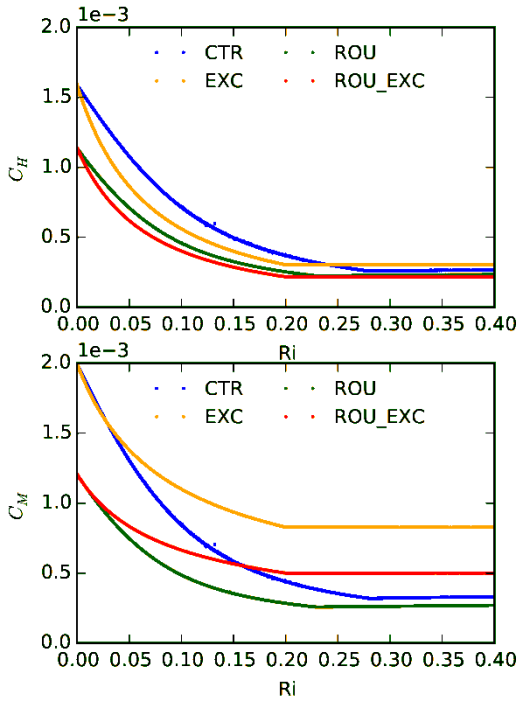

Figure S 1. Heat (top) and momentum (bottom) transfer coefficients as a function of the Richardson Number: default IFS configuration (CTR, blue), default IFS configuration with lower roughness lengths (ROU, green), SURFEX formulation with IFS roughness lengths (EXC: organge) and SURFEX formulations with lower roughness lengths (ROU_EXC).

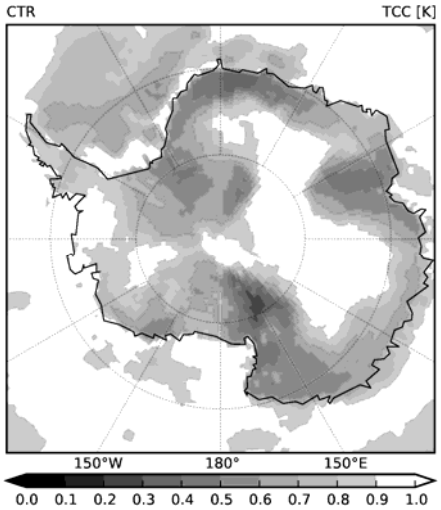

Figure S 2. Total cloud cover in the control experiment.

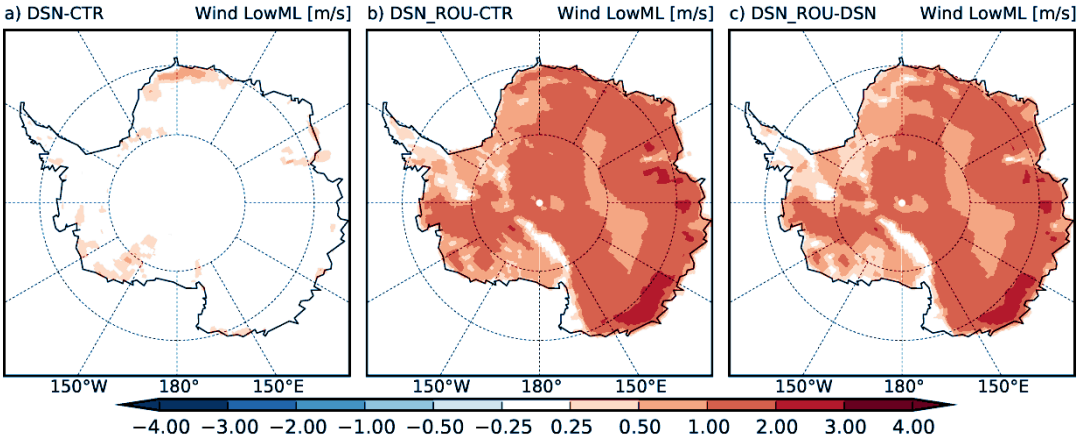

Figure S 3. Impact on the lowest model level wind speed.

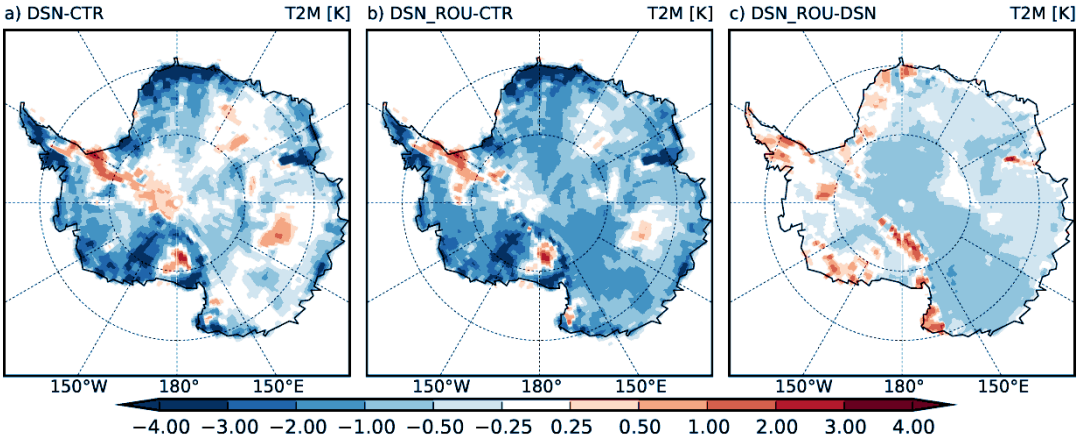

Figure S 4. Impact on 2-meter temperature.

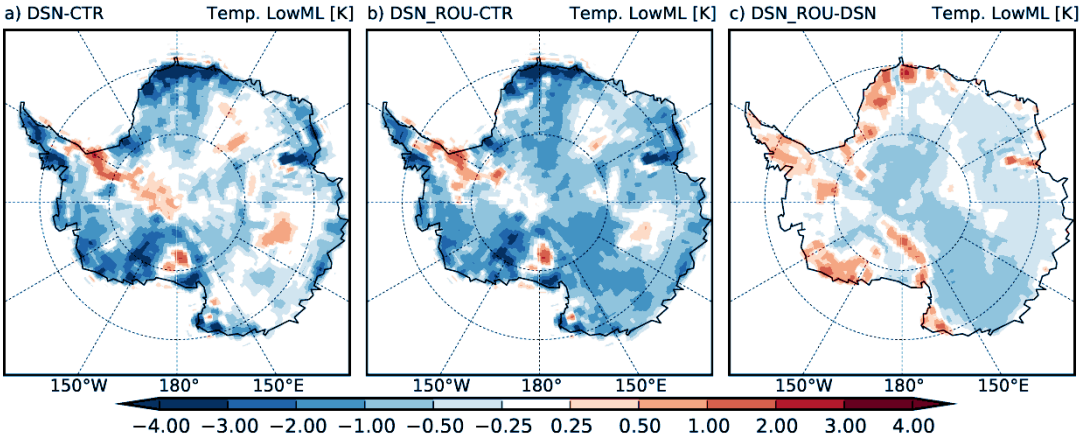

Figure S 5. Impact on the lowest model level temperature.